



HAL
open science

On the importance of precise measurements of the optical properties of gold electrodes in LIMM/(F)LIMM

Flora Carrasco, Kremena Makasheva, Didier Marty-Dessus, Laurent Berquez

► To cite this version:

Flora Carrasco, Kremena Makasheva, Didier Marty-Dessus, Laurent Berquez. On the importance of precise measurements of the optical properties of gold electrodes in LIMM/(F)LIMM. Conference on Electrical Insulation and Dielectric Phenomena (CEIDP), Dec 2021, Vancouver, Canada. pp.627-630, 10.1109/CEIDP50766.2021.9705373 . hal-03578965

HAL Id: hal-03578965

<https://hal.science/hal-03578965>

Submitted on 17 Feb 2022

HAL is a multi-disciplinary open access archive for the deposit and dissemination of scientific research documents, whether they are published or not. The documents may come from teaching and research institutions in France or abroad, or from public or private research centers.

L'archive ouverte pluridisciplinaire **HAL**, est destinée au dépôt et à la diffusion de documents scientifiques de niveau recherche, publiés ou non, émanant des établissements d'enseignement et de recherche français ou étrangers, des laboratoires publics ou privés.

On the importance of precise measurements of the optical properties of gold electrodes in LIMM/(F)LIMM

Flora Carrasco

LAPLACE, Université de Toulouse,
CNRS, UPS, INPT, Toulouse, France
carrasco@laplace.univ-tlse.fr

Kremena Makasheva

LAPLACE, Université de Toulouse,
CNRS, UPS, INPT, Toulouse, France
makasheva@laplace.univ-tlse.fr

Didier Marty-Dessus

LAPLACE, Université de Toulouse,
CNRS, UPS, INPT, Toulouse, France
marty@laplace.univ-tlse.fr

Laurent Berquez

LAPLACE, Université de Toulouse,
CNRS, UPS, INPT, Toulouse, France
berquez@laplace.univ-tlse.fr

Abstract— Precise measurements of the optical properties of electrodes add value to the interpretation of the recorded current spectra when applying Laser Intensity Modulation Method (LIMM) for space charge density measurements, including also its version with focused laser ((F)LIMM). They allow to correctly account for the energy deposition in the metal electrode and in the dielectric material under study. In this work the refractive index (n) and the extinction coefficient (k) have been extracted from the recorded by spectroscopic ellipsometry spectra and then integrated in the model to account for the nature and real conditions of the electrode. Such approach improves modeling of the temperature required for extraction of the space charge. It is found that higher refractive indexes of the gold electrodes lead to an important increase of the signal/noise ratio, thus improving the sensibility of the method for space charge measurements. It also allows to probe much lower levels of space charge densities.

I. INTRODUCTION

Performance and reliability of solid dielectric materials under electrical stress are tightly linked to the behaviour of charge carriers present in the dielectric [1]. The origin of these internal charges, so-called space charge, is generally considered twofold. One finds (*i*) intrinsic charges, having as a source charge injection from the contact between the electrodes and the material, charge generation in the bulk due to electro-dissociation of weakly-bounded ionic species and (*ii*) extrinsic ones, relying on charge implantation upon irradiation, by ionizing radiation, *e.g.*, space environment conditions, or exposure to partial discharges. In some applications the space charge is used to convey specific electrostatic properties to the dielectric material resulting from the charge deep trapping, like for example in the case of electret-based microphones [2], in non-volatile memories [3, 4], etc. In other applications, the space charge build-up represents an enormous drawback, entailing the risk to develop to a breakdown, like for example the high voltage DC (HVDC) cables with polymeric insulation [5–9]. Regardless the source of space charge, an adequate description of charge injection, localization and charge transport in dielectric materials is a requirement to better

understand the behaviour of insulating materials under electrical stress. To that end various diagnostic methods have been developed during the years of intensive scientific and technological research, aiming at achieving, among others, a high resolution in the analysis of space charge distribution in solid dielectrics [1, 5, 7–12].

One of the quite frequently used methods for space charge diagnostic, especially for polymeric insulation materials, is Laser Intensity Modulation Method (LIMM) [10, 11], including its version with focused laser ((F)LIMM) [12]. The LIMM/(F)LIMM is a thermal wave based method which uses a modulated laser beam to heat the surface sample. The laser beam energy is absorbed by the electrode and the sample is then subjected to a temperature variation on its face. The diffusion of heat through the sample expands the material in a non-uniform manner, causing charges displacement and local variation of the dielectric constant. These two mechanisms induce an electrical response of the insulating material *i.e.*, a current flowing between the electrodes of the sample. A Fredholm equation of first kind links the measured current to the space charge density and the temperature distribution which is modeled [13]. The precise knowledge of the temperature distribution in the sample is then of major importance as it controls the accuracy of the space charge profiles to be determined.

For the (F)LIMM-variant of the method, the laser beam is focused, allowing thus a three-dimensional space charge mapping. The spatial resolution of these maps is inversely proportional to the electrode thickness. So, in order to improve accuracy in the analysis of the recorded current, information on the optical properties of the metal electrodes under real conditions is essential.

As mentioned above, the mode of operation of the LIMM/(F)LIMM diagnostic methods involves metal electrodes. Due to some peculiarities related to the extraction of their optical properties during space charge measurements, their influence is often neglected in the applied methodology for processing of the recorded signal. The aim of this contribution

is to shed a light on the importance of precise measurements of the optical properties of the metal electrodes in space charge measurements by LIMM/(F)LIMM.

II. EXPERIMENTAL PART

A. Description of the gold electrodes

The electrodes under study are made from gold. They are sputtered on spin-coated polyimide films on silicon wafers. They are with thicknesses in the range 50 – 200 nm, with the latter measured at the sputtering step. To represent the evolution of the optical properties of gold electrodes as a function of the thickness, three electrodes with thickness of 50, 150 and 200 nm, called hereafter Sample A, B and C, respectively, are discussed in this contribution.

B. Spectroscopic ellipsometry: Principal of operation and spectra modeling

The optical parameters of the golden electrodes (refractive index, n and extinction coefficient, k) are obtained in this work after processing of the recorded spectra, by spectroscopic ellipsometry (SE), in the UV-Vis-NIR range (250 – 850 nm) with 5 nm resolution. A Semilab ellipsometer SE-2000 with a rotating polarizer and a fixed analyzer is used. To increase the accuracy light beam incident angle of $\Theta = 69^\circ$ is applied, as found the most appropriate angle value for gold bulk materials [14]. The measurements are performed at room temperature.

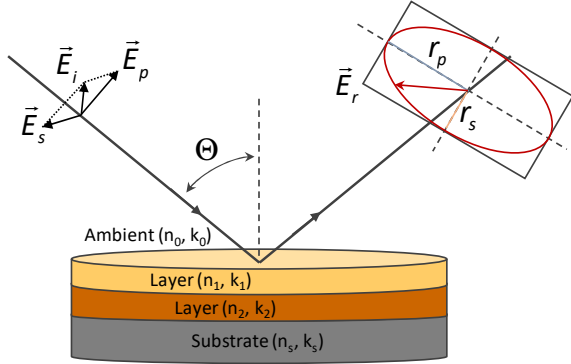


Fig. 1. Schematic representation of the principal of operation of spectroscopic ellipsometry.

SE is an optical technique based on measurements of the changes in polarization of a monochromatic plane wave occurring upon reflection at oblique incidence (Fig. 1) [15]. SE is a non-destructive, low-cost and easy to apply diagnostic method. It is appropriate for *in-situ* and *ex-situ* measurements of the thicknesses and the optical properties of thin transparent layers or for extraction of the optical properties of bulk materials. The latter option is applied in this work.

The basic quantity measured with SE is the complex reflectance ratio ρ . For optically isotropic samples the expression for ρ simplifies to eq. (1) where r_p and r_s are the complex reflection coefficients for light polarized parallel and perpendicular to the plane of incidence, respectively:

$$\rho = \frac{r_p}{r_s} = \left| \frac{r_p}{r_s} \right| e^{i(\delta_s - \delta_p)} = \tan(\Psi) e^{i\Delta}. \quad (1)$$

The directly measured quantities in SE are $\tan(\Psi)$ and $\cos(\Delta)$, where Ψ and Δ are called ellipsometric angles. In particular, $\tan(\Psi)$ represents the ratio between the moduli of the reflection coefficients (eq. (1)), meaning that it is closely related to the changes in the amplitudes of the polarized electric field after reflection. The $\cos(\Delta)$ gives the phase difference ($\Delta = \delta_p - \delta_s$) between the perpendicular (δ_s) and parallel (δ_p) components of the polarized electric field, induced by the reflection (Fig. 1). It is worth pointing out that as an indirect technique, the SE requires an appropriate optical model to extract the desired information. For determining the complex refractive index, $\tilde{n} = n + ik$ of bulk materials, like for the gold electrodes here, the complex reflectance ratio ρ is converted into pseudo dielectric function and n and k are extracted from its relation with the parallel and perpendicular components of the polarized electric field.

C. Experimental set-up for LIMM/(F)LIMM measurements

The (F)LIMM general principle and conventional set-up have been already described in [16], whereas its modifications towards an on-line equipment were recently detailed in [17]. Figure 2 shows a scheme of the experimental set-up. A DC potential (V_{ht}) is applied to the top electrode of the measuring cell. The laser beam (MPT35 – 35 mW, 658 nm) modulated between 10Hz and 10kHz is used to heat the sample. (F)LIMM currents are recorded after pre-amplification (FEMTO LCA-200K) and extracted from noise by a lock-in amplifier (EG&G-5302).

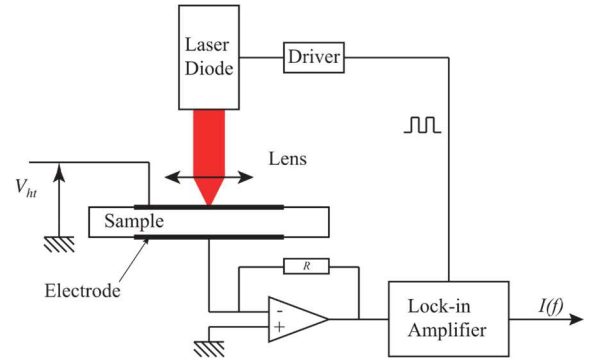


Fig. 2. (F)LIMM set-up.

The recorded current spectra are then proceeded according a deconvolution algorithm. The latter allows to access the space charge density at a given depth in the probed insulating sample.

III. RESULTS AND DISCUSSION

The recorded SE spectra of the three electrodes (Sample A, B and C) are reported in Fig. 3. They have the typical, for gold, shape in the studied spectral range. The non-monotonic behaviour of the SE spectra of Sample A for wavelengths higher than 500 nm (photon energy lower than 2.5 eV) is due to the transparency of the electrode defined by the small thickness, of only 50 nm. One actually observes the variations induced by the underlying polyimide film. This undesirable effect would lead to an impossibility to model the temperature and thus,

would induce misinterpretation of the recorded current spectra and inaccuracy in the results for the space charge distribution. For the rest of our analysis Sample A will be omitted since it is not possible to assess the transmitted fraction of the polarized light which in turns prevents from accurate extraction of the complex index of refraction $\tilde{n} = n + ik$.

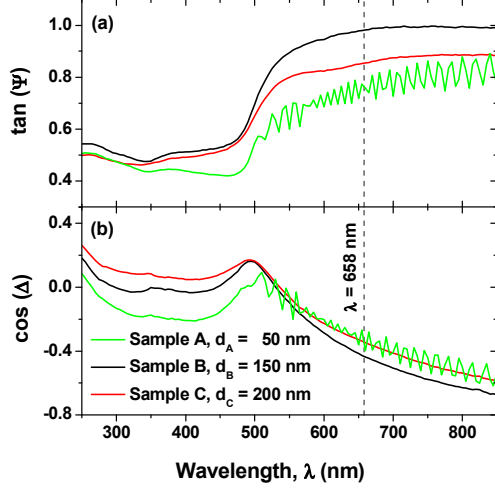


Fig. 3. Recorded SE spectra for the three Au-electrodes: $\tan(\Psi)$ on (a) and $\cos(\Delta)$ on (b). The wavelength of the laser ($\lambda = 658$ nm) used in the LIMM measurements is shown in dashed-line.

The extracted (from SE spectra) optical properties (n and k) of the two samples are shown in Fig. 4. The obtained values at the wavelength of the laser beam ($\lambda = 658$ nm) used for LIMM measurements are reported in Table 1. Given that the real ϵ_r ($\epsilon_r = n^2 - k^2$) and imaginary parts ϵ_i ($\epsilon_i = 2nk$) of the complex dielectric constant $\tilde{\epsilon} = \epsilon_r + i\epsilon_i$ are closely related to the electronic structure of the materials they are more convenient for a use dealing with application purposes. However, for more clarity, the following analysis is presented in terms of $\tilde{n} = n + ik$, where $\tilde{\epsilon} = \tilde{n}^2$, and gives the relation with the complex dielectric function of the material.

Table 1. Summary of the obtained values of the refractive index, extinction coefficients and absorption coefficients at $\lambda = 658$ nm.

	Sample B	Sample C
Refractive index, n	0.09	0.6
Extinction coefficient, k	3.7	3.3
Absorption coefficient β (m^{-1})	7.1×10^7	6.3×10^7

The obtained optical properties (n and k) of the used gold electrodes are in accordance with previously reported values in the studied spectral range, those of Sample C being closer to the reported ones in the literature [14, 18]. One can notice significant variations mainly in the Vis-NIR range for wavelengths higher than 500 nm for both the refractive index and the extinction coefficient (Fig. 4). Such tendency is clearly a sign of reorganization of the material, in particular its densification. Two reasons appear to be the most probable for such an evolution: material thickness and thermally induced modifications. As far as the former one, the effect of thickness on the evolution of the optical properties was reported for gold

electrodes of thicknesses lower than 30 nm. So, most likely in the case of Sample C, a thermally induced reorganization/densification of the metal electrode occurred. It led to an increase of n in this wavelength (energy) range [14]. Accurate determination of the optical constants in this part of the spectrum is critical for space charge measurements by LIMM/(F)LIMM methods, since the laser beam is in the same spectral range ($\lambda = 658$ nm). Moreover, the free-electron effects play a dominant role in the NIR-spectral range.

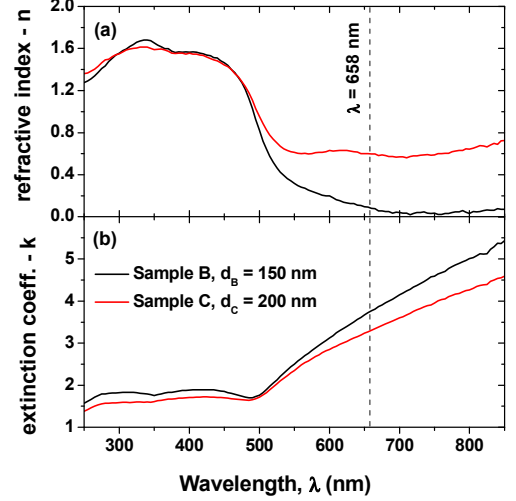


Fig. 4. SE extracted spectra of the refractive index, n on (a) and the extinction coefficient, k on (b), for Samples B and C.

In the modeling part of the LIMM/(F)FLIMM diagnostic method one enters the absorption coefficient (β , Fig. 5(a), Table 1) is used as parameter. Its value is obtained from the SE spectra, since for a given wavelength, the absorption coefficient is proportional to the extinction coefficient:

$$\beta = \frac{4\pi k}{\lambda}. \quad (2)$$

It also allows to estimate the penetration depth of the laser beam (Fig. 5(b)), limited to only 23 nm in the studied gold electrodes.

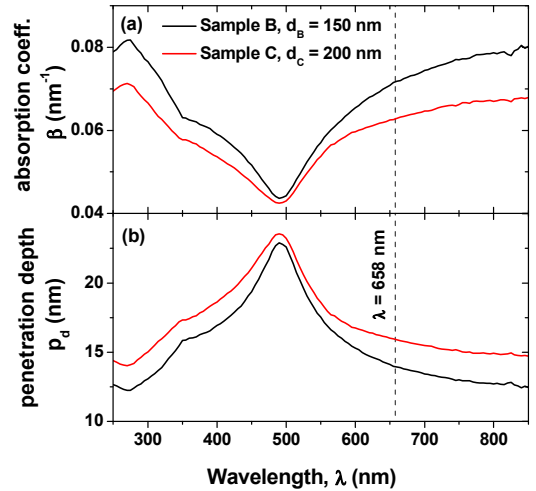


Fig. 5. Absorption coefficient, β (a), and penetration depth, p_d (b), of the light beam in the gold electrodes, as obtained from the SE spectra.

Figure 6 gives the real and imaginary parts of the LImm currents for Samples B and C when submitted to an electric field of 25 kV/mm. The current measured for Sample C is six times higher than the one measured for sample B. This is directly related to the values of the gold electrode optical constants, given in Table 1. The extracted refractive index, n at the laser wavelength for Sample B leads to a reflection of 98% of the laser beam. For sample C, this percentage is much lower, 82%. Hence, a much higher fraction of the laser beam energy is absorbed in Sample C (18%), compared to Sample B (only 2%), and thus converted to a heat. This means that for Sample C the thermal wave to probe the insulating material is produced with eight times more energy. As a consequence, the measured current is much higher (Fig. 6) giving the possibility to probe smaller amount of space charge.

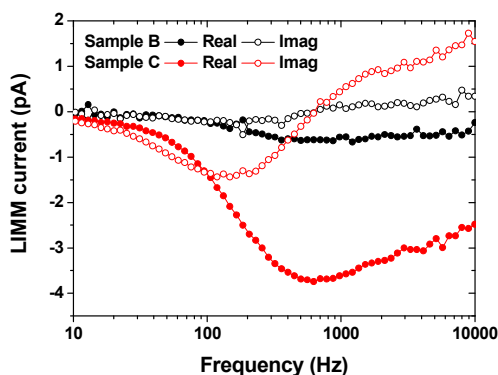


Fig. 6. Real part and imaginary part of the LImm currents for Samples B and C submitted to electric field of 25 kV/mm.

The above example shows that the knowledge of the optical properties of the metal electrodes allows to assess the energy deposition in order to accurately model the temperature distribution, and consequently to precisely extract the space charge density in LImm/(F)LImm.

IV. CONCLUSION

By this contribution we have shown as how precise measurements of the optical properties of the metal electrodes in LImm/(F)LImm diagnostic methods improve their sensitivity, in terms of current measurements. As a consequence, a lower level of space charge would be accessible. Other benefit of this approach can be found in the improved signal to noise ratio. Thus the accuracy in extraction of the space charge density can be increased. Based on the performed analysis one can conclude that such an approach should be applied to all techniques of space charge measurements involving laser light through metal electrodes.

In the future, this study will be applied to other types of metal electrodes. A specific attention will be paid to the variation of optical properties of the metal electrodes induced by the environment, like for example, oxidation, contamination and/or humidity.

- [1] L. A. Dissado and J. C. Fothergill, *Electrical degradation and breakdown in polymers*. London: P. Peregrinus, 1992.
- [2] G. M. Sessler, "Electrets: recent developments," *J. Electrostat.*, vol. 51–52, pp. 137–145, May 2001.
- [3] E. Kapetanakis *et al.*, "Charge storage and interface states effects in Si-nanocrystal memory obtained using low-energy Si⁺ implantation and annealing," *Appl. Phys. Lett.*, vol. 77, no. 21, pp. 3450–3452, Nov. 2000.
- [4] S. Perret-Tran-Van, K. Makasheva, B. Despax, C. Bonafos, P. E. Coulon, and V. Paillard, "Controlled fabrication of Si nanocrystals embedded in thin SiON layers by PPECVD followed by oxidizing annealing," *Nanotechnology*, vol. 21, no. 28, p. 285605, Jul. 2010.
- [5] T. J. Lewis, "Polyethylene under electrical stress," *IEEE Trans. Dielectr. Electr. Insul.*, vol. 9, no. 5, pp. 717–729, Oct. 2002.
- [6] J. P. Jones, J. P. Llewellyn, and T. J. Lewis, "The contribution of field-induced morphological change to the electrical aging and breakdown of polyethylene," *IEEE Trans. Dielectr. Electr. Insul.*, vol. 12, no. 5, pp. 951–966, Oct. 2005.
- [7] G. C. Montanari and P. H. F. Morshuis, "Space charge phenomenology in polymeric insulating materials," *IEEE Trans. Dielectr. Electr. Insul.*, vol. 12, no. 4, pp. 754–767, Aug. 2005.
- [8] T. D. Huan *et al.*, "Advanced polymeric dielectrics for high energy density applications," *Prog. Mater. Sci.*, vol. 83, pp. 236–269, Oct. 2016.
- [9] G. Teyssedre, S. T. Li, K. Makasheva, N. Zhao, L. Milliere, and C. Laurent, "Interface tailoring for charge injection control in polyethylene," *IEEE Trans. Dielectr. Electr. Insul.*, vol. 24, no. 3, pp. 1319–1330, Jun. 2017.
- [10] S. B. Lang and D. K. Das-Gupta, "A technique for determining the polarization distribution in thin polymer electrets using periodic heating," *Ferroelectrics*, vol. 39, no. 1, pp. 1249–1252, Oct. 1981.
- [11] S. B. Lang and D. K. Das-Gupta, "A new technique for determination of the spatial distribution of polarization in polymer electrets," *Ferroelectrics*, vol. 60, no. 1, pp. 23–36, Oct. 1984.
- [12] D. Marty-Dessus, L. Berquez, A. Petre, M. Mousseigne, and J. L. Franceschi, "Three-dimensional cartography of space charge by FLImm," in *Annual Report Conference on Electrical Insulation and Dielectric Phenomena*, Cancun, Mexico, 2002, pp. 602–605.
- [13] A. Velazquez-Salazar, L. Berquez, and D. Marty-Dessus, "Thermal modeling and calibration in (F)LImm using an external bias field: Theory and experiment," *IEEE Trans. Dielectr. Electr. Insul.*, vol. 25, no. 3, pp. 783–790, Jun. 2018.
- [14] C. Villeneuve-Faure *et al.*, "Kelvin force microscopy characterization of charging effect in thin a-SiO_xN_y:H layers deposited in pulsed plasma enhanced chemical vapor deposition process by tuning the Silicon-environment," *J. Appl. Phys.*, vol. 113, no. 20, p. 204102, May 2013.
- [15] H. G. Tompkins and E. A. Irene, Eds., *Handbook of ellipsometry*. Norwich, NY : Heidelberg, Germany: William Andrew Pub. ; Springer, 2005.
- [16] D. Marty-Dessus, A. C. Ziani, A. Petre, and L. Berquez, "Space charge distributions in insulating polymers: A new non-contacting way of measurement," *Rev. Sci. Instrum.*, vol. 86, no. 4, p. 043905, Apr. 2015.
- [17] A. Velazquez-Salazar, L. Berquez, and D. Marty-Dessus, "Towards space charge measurements by (F)LImm under DC electric field," in *2016 IEEE International Conference on Dielectrics (ICD)*, Montpellier, France, Jul. 2016, pp. 223–226.
- [18] P. B. Johnson and R. W. Christy, "Optical Constants of the Noble Metals," *Phys. Rev. B*, vol. 6, no. 12, pp. 4370–4379, Dec. 1972.